RSC Advances

ROYAL SOCIETY OF CHEMISTRY

www.rsc.org/advances

Effect of zeolite on SPEEK /zeolite hybrid membrane as electrolyte for microbial fuel cell applications

Narayanaswany Venkatesan Prabhu and Dharmalingam Sangeetha*

Department of Mechanical Engineering, Anna University, Chennai – 25, Tamil Nadu, India.

**Corresponding Author. Tel: +91 044 22357763.*

E-mail address: sangeetha@annauniv.edu

Abstract:

Zeolite (H-Faujasite) incorporated SPEEK membrane was demonstrated as an effective proton exchange membrane for Microbial Fuel Cell (MFC) application. The proton conductive faujasite zeolite contains uniform channels with an effective diameter ~ 0.74nm that permits small ions but restricts large hydrated ions. In this work, SPEEK/Zeolite membranes were prepared by solvent evaporation method with different weight percentages (2.5%, 5%, 7.5%, 10%) of zeolite. The physico-chemical properties of the composite membranes such as water uptake, ion-exchange capacity, proton conductivity, dissolved oxygen crossover and transport of cations were studied for its suitability in MFC. A maximum proton conductivity of 0.178 X 10^{-2} S cm^{-1} was obtained for 7.5 % Zeolite + SPEEK. All the membranes were tested in a Single Chamber MFC (SCMFC) using *E.coli* inoculum and Pt/C as cathode catalyst. 7.5 % Zeolite + SPEEK membrane showed the highest power density (176mW/m^2) than that of commercial Nafion and other composite membranes.

Keywords: Faujasite, sulfonated poly (ether ether ketone), Hydrated ions, Cations transport, Microbial Fuel Cell performance.

1. Introduction

Microbial Fuel Cell (MFC) has achieved a remarkable place among renewable energy technology, because of its mode of electricity generation from degradable waste materials. Functioning of MFC is similar to that of chemical fuel cell. One of the main differences between MFCs and other chemical fuel cells is with respect to the anode catalyst. The anode catalysts of chemical fuel cells are commonly Pt and Pt based compounds whereas the anode catalysts of MFCs are microorganisms that are called biocatalysts[1].

In a simple description, a dual chamber MFC consists of anodic and cathodic chambers separated by a polymer electrolyte membrane (PEM). In anaerobic anodic chamber, microorganisms that act as biocatalyst oxidize degradable waste into proton and electron **mean**while in cathodic chamber where dissolved oxygen, potassium permanganate or potassium ferricyanide is used as electron acceptor. PEM is used to avoid mixing of the two compartment solutions and keep the anodic chamber as oxygen free as possible [2–6].

MFC functioning is based on the electrons, protons produced by microorganisms from the oxidation of degradable waste materials. In the absence of oxygen in anodic chamber, micro-organisms transfer electrons to the anode electrode of MFC[7]. The oxidation of substrate (glucose) by microorganisms yields 24 protons and electrons for functioning of MFC.

$$C_6H_{12}O_6 + 6H_2O \rightarrow 6CO_2 + 24H^+ + 24e^-$$

These produced electrons are used when they pass through a load in the external circuit, and eventually reduce electron acceptors at cathode electrode and combines with the proton that reaches the cathodic chamber through the PEM from anodic chamber, which finally results in the formation of water.

Even though, working of single chamber MFC (SCMFC) is similar to dual chamber MFC, it has more advantages over dual chamber MFC [8,9], since no separate cathodic chamber is needed like in dual chamber MFC. A SCMFC consists of anaerobic anodic chamber, PEM and air-facing cathode attached with the PEM. Pt/C (for cathode alone) is coated in cathode electrode and it is used to reduce oxygen which acts as electron acceptor in SCMFC instead of potassium permanagate, ferricyanide as used in dual chamber MFC [10–15]

Effective operation of MFC requires an electrolyte membrane separator to separate the chemical reaction at anode from cathode both chemically and electrically. An effective membrane must possess its own potential in terms of oxygen crossover, ion exchange capacity, water uptake and proton conductivity, which are well connected with MFC's higher power density output[16]. The most widely used commercial electrolyte membrane in fuel cells is perfluorinated Nafion® due to its high proton conductivity property. Apart from its high cost and fluorinated polymer backbone, Nafion possesses several drawbacks especially for its application in MFC such as high oxygen crossover, substrate loss and transport of cations other than protons, which are present in microbial inoculum. It is also used in the form of polymer coating over cathode surface in MFC to study the property of MFC [17,18].

Several hybrid non fluorinated membranes with or without ion exchangeable groups such as glass fiber, J-Cloth, nylon, Teflon coated layers are used as separators in MFC replacing Nafion, whose properties were studied and tested in MFC. Even though, these separators are cost effective alternatives for Nafion, they have major shortfalls of higher oxygen crossover, substrate loss (low columbic efficiency) and accumulation of cations other than proton, which affects the power generation since high power density is achieved only under highly anaerobic anodic condition with good proton conductivity [19].

Recent studies have been focused on utilizing composite membranes because of their better properties, performance and lower price[20,21]. The sulfonated polyether ether ketone/polyether sulfone[20], Polyether sulfone/Fe_3O_4[22],sulfonated fullerene/sulfonated polyether ether ketone[23] and sulfonated polyether ether ketone/Graphene oxide[24] have shown better performance than Nafion membrane in MFC applications. Nafion modified with activated carbon nanofiber [25] and PVDF[26] membranes have produced higher power densities than their original Nafion membrane in MFC. The addition of fillers improves the ionic conductivity; reduces oxygen crossover and transport of cations other than protons by creating preferential path. The studies[16,18,20,21,27] showed that non-fluorinated hybrid membranes based on sulfonated poly (ether ether ketone) (SPEEK)[17,28] have been described as high potential materials in MFC due to their better properties compared to that of Nafion membranes.

Among inorganic fillers, zeolites are porous, crystalline, hydrated microporous aluminosilicate minerals of alkali and alkaline earth cations characterized by an ability to exchange some of their constituent cations with aqueous solutions, without a major change in structure [29]. They have three-dimensional structures arising from the coordination of silicate ($[SiO4]^{4-}$) and aluminate ($[AlO4]^{5-}$) tetrahedral linked by all corners [30]. In addition, their properties are mostly dependent on the Si/Al ratio of their structures. Because of their ion-exchange, adsorption, and molecular sieve properties, as well as their geographically widespread abundance, zeolite minerals have generated worldwide interest for use in a broad range of applications including fuel cells [31], [32]. Being porous, water molecules present in zeolite cage favor the movement of protons through water mediated proton transfer and in turn the conductivity of membranes get increased with the incorporation of zeolites. Hence, zeolites are used for improving the performance of membrane [32].

In this present work, the potential use of Faujasite (FAU) type zeolites as filler material for fuel cell electrolyte was studied and evaluated in MFC. The poor acidic stability of Faujasite is a drawback of its use in acidic fuel cells, however its use in MFC is much appreciable since MFC operates in neutral pH. Apart from the stability in acidic medium, FAUs were chosen for their large pore size (7.4 Å), high surface area, an open three dimensional pore system, and for their commercial availability in a wide range of chemical compositions [33]. The present work reports on the preparation and characterization of SPEEK–Faujasite zeolite composite membranes for MFC. Faujasite-type zeolites were used as fillers to result in much faster intracrystalline diffusion rates compared to other zeolites [34,35]. In particular, the Faujasite zeolite (H form) has been used in this work to facilitate the interaction with polymer matrix [36]. This study investigates the ion exchange capacity, water uptake, proton conductivity and cation transport of the zeolite composite membranes for MFC application.

2. Materials and method:

The materials used in the study were procured commercially from different sources. PEEK (Mol. Wt. 1,00,000), Conc. H_2SO_4, D – Glusose, Ethanol, Nutrient medium and N-Methyl Pyrollidone (NMP) were purchased from Victrex, Merck, Sigma Aldrich, Sigma Aldrich, SRL and SRL respectively. All the chemicals were used for the study without any further purification. Zeolite Y Hydrogen (Faujasite – "H" Form) was purchased from Alfa Aesar.

2.2 Sulfonation of PEEK and composite membrane preparation:

PEEK polymer was sulfonated using sulfuric acid as sulfonating agent. The weighed amount of PEEK was dissolved in concentrated sulfuric acid and magnetically stirred for five hours. After 5 hours, the reaction mixture was poured into cold water and the sulfonated PEEK (SPEEK) was obtained in the form of white precipitate. The SPEEK was washed with deionized

water for several times until the pH becomes neutral. The SPEEK obtained from the above process was dried in a vacuum oven at 80°C overnight. It was then dissolved in a suitable quantity of NMP and cast onto a clean, dry petri dish. The membrane was obtained by evaporating the solvent in vacuum oven at 80°C for 24 hours. The obtained membranes were pale brown in color and were peeled off from the dish and stored for further analysis. The reaction scheme is given below [37].

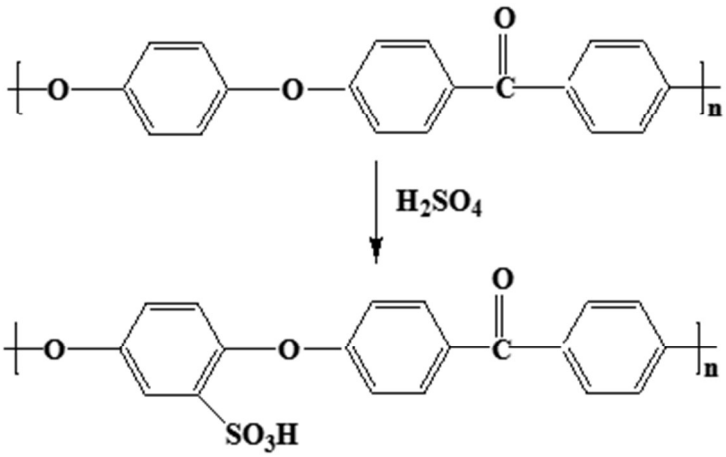

The SPEEK ionomer was dissolved in the NMP solvent and different proportions of zeolite were added to the solution, stirred for 24h, and subsequently ultrasonicated for about 15 min, followed by casting into a clean dried petri dish to obtain membrane of the required thickness. The cast membrane was dried at 80^{o} C for 24 hours.

Composite membranes of SPEEK with different weight percentages (2.5%, 5%, 7.5% and 10%) of zeolites were fabricated and characterized using the following techniques.

2.3 Instrumental Characterizations:

2.3.1 Fourier Transform Infrared Spectra (FTIR):

The prepared composite membranes were characterized using ATR- Fourier Transform Infrared spectrometer (Alpha T-Bruker Optics) for the presence of functional groups. The membranes were scanned in ATR mode from the wavenumber of 400cm^{-1} – 4000cm^{-1}.

2.3.2 X- ray Diffraction (XRD):

The crystalline nature of the polymer composite membranes was studied using XRD. XRD measurements were performed using an X' Pert Pro PAN analytical powder XRD. The scanning angle was from 1° - 80° with a scanning rate of 2° per min.

2.3.3 SEM:

The surface morphology of the composite membranes and dispersion of zeolite on the membranes were studied using VEGA3 TECSCAN Scanning Electron Microscope (SEM) at an accelerating voltage of 15 kV and a resolution of 5 μm. Prior to SEM analysis, the samples were dried and then coated with gold by sputtering.

2.3.4 Proton Conductivity:

Proton conductivity of the membranes was studied using electrochemical impedance spectrometer (Biologics VSP, France). The membranes were sandwiched between two brass rods, which were supported on an acrylic plate. The two-electrode method was used to study the proton conductivity of the composite membrane using Z fit software.

$$\text{Conductivity (S/cm)} = \frac{L}{(R \times A)}$$

Where, R = Sample resistance, Ω, L = Wet sample thickness, cm, and A=Sample area, cm^2.

2.3.5 Water uptake:

Water uptake of the composite membranes was studied by change in the weight of the composite membranes before and after hydration. Before the experiment, the membranes were dried well in a hot air oven and then taken for the study. The percentage of water absorption was calculated using the relation given below.

$$\% \text{ water absorption} = \frac{\text{wt. of wet polymer-wt. of dry polymer}}{\text{wt. of dry polymer}} \text{ X } 100$$

2.3.6 Ion exchange capacity (IEC):

Ion exchange capacity is a measure of the ability of an insoluble material to undergo displacement of ions previously attached and loosely incorporated into its structure by oppositely charged ions present in the surrounding solution. IEC is generally determined by volumetric method. The greater the ion exchange capacity better will be the proton conductivity of the membrane. Ion exchange capacity is directly dependent on the number of sulfonic acid groups present in the sulfonated polymer. The sulfonated membranes and composite membranes were soaked in the 2M KCl solution for 24 hours to saturate the membranes and the protons released by the membranes were neutralized by sodium carbonate solution of known concentration with phenolphthalein as indicator. IEC was calculated by using the formula given below

$$\text{IEC} = \frac{\text{Titre value(in ml)X Normality of } Na_2CO_3}{\text{weight of dry polymer membrane(in g)}} \text{ meq/g}$$

2.3.7 Dissolved oxygen cross over:

The oxygen mass transfer coefficient of fabricated composite membrane was studied using a portable dissolved oxygen (DO) probe (Extech 407510A, Taiwan). For the determination of oxygen mass transfer coefficient, a two chambered bottle MFC was used as described earlier [38] to find out the oxygen mass transfer for each membrane using uninoculated bottle-MFC reactors and nutrient medium. The cathode chamber was continuously aerated to maintain saturated dissolved oxygen (DO) conditions. A dissolved oxygen (DO) probe was placed in the nitrogen saturated completely sealed anode chamber. The oxygen mass transfer coefficient was calculated [38] (as per Olivier et al., 2011) from DO concentration over a period of 10h. The study showed the resistance of PEM separator to oxygen permeability, which affects the anaerobic atmosphere of the anodic chamber.

2.3.8 Surface roughness:

The surface roughness of the membranes was studied using a 3D Non-contact profilometer (Taylor Hobson hardness tester) and the respective average roughness (Ra) values were calculated using TalyMap Platinum 5.1.1.5374 software.

2.3.9 Determination of cations transport through membrane:

Membrane's cation transport study was carried out according to the procedure reported by Rozendal et al [39]. Initially 20 mM sodium, 25 mM potassium, 5.2 mM ammonium, 0.7 mM calcium, and 0.4 mM magnesium containing synthetic wastewater was chosen for the study. Cation species (Na^+, K^+, Ca^{2+}, and Mg^{2+}) concentrations were determined using inductively coupled plasma-optical emission spectroscopy (ICP-OES; Perkin- Elmer Optima 3000XL). Ammonium ion concentrations were determined by Phenate method using UV-Visible spectrophotometer at 640 nm. In order to study the cation transport through the membranes, a dual chamber MFC setup [40] with anode and cathode chambers was used to observe the transport of cations from the anode chamber to the cathode chamber

2.3.10 MFC Construction and Operation:

The fabricated MFC consisting of an acrylic cylindrical chamber 4 cm long and 3 cm in diameter (empty bed volume of 28 ml) was separated by a proton exchange membrane and *E coli* were used as bacteria in the anodic chamber. The anode electrode was prepared using 30% wet proofed carbon cloth (Cabot carbon Inc from, Germany) and then carbonized using Vulcan X C - 72 (Arora Mathey, Kolkata) (3mg/cm^2) with 30% of PTFE (Sigma Aldrich, India) and appropriate amount of double distilled water and Isopropyl alcohol (SRL, India). The carbon cloth was then heat-treated for three hours at 250 ^oC. The carbonized carbon cloth was used as anode electrode. For the cathode electrode, the same procedure was followed with an amount of 0.5mg/cm^2 Pt/C (Arora Mathey, Kolkata) and was brush coated on the carbonized carbon cloth

and dried at 200 ^{o}C for 5 h. The catalyst coated carbon cloth was then hot pressed on the membrane at 80 ^{o}C with 1.5 ton pressure for 3 min to obtain the Cathode Electrode Assembly (CEA). The surface areas of both anode and cathode were 7.07 cm^2.

E coli strains (DH5-α) [41–43] from our pre adapted laboratory culture collection were used and the bacterial culture was enriched by purging nitrogen gas and kept in shaker for 48 hours. The anode chamber was filled with the enriched *E coli* nutrient medium and the chamber was continuously flushed with N_2/CO_2 (80:20) to maintain anaerobic conditions as well as the pH of the growth medium at 7.

The bacterium containing inoculum in anodic chamber was changed 3–5 times (i.e., over 72–120 h) to allow a biofilm to form on the anode surface. The chamber was refilled each time when the voltage reached a minimum value [44].

2.3.11 Fuel Cell Analysis:

The Coulombic Efficiency (CE) was calculated using the following equation.

$$CE\ (\%) = \frac{C_P}{C_T} \text{ X } 100$$

Where, C_P is the total Coulombs calculated by integrating the current over time. C_T is the theoretical amount of Coulombs that can be produced from glucose and is calculated as

$$C_T = \frac{FbSv}{M}$$

Where, F is Faraday's constant (98485 C/mol of electrons), b is the number of mol of electrons produced per mol of substrate (glucose) (b = 24), S (g/L) is the substrate (glucose) concentration, v (mL) the liquid volume and M the molecular weight of the substrate (glucose) (M = 180).

The values of cell voltage and current were observed and recorded, using a precision digital multimeter (Model 702, Metravi, India). The circuit was completed with a resistor of 1 kilo ohms except when different resistors (100 ohms to 1000 ohms) were used to determine the power generation as a function of load. The power density values were obtained after a stable voltage was obtained. The current was calculated using Ohm's law

$$I = V/R$$

where, I (mA) is the current, V (mV) is the voltage and R is the external resistance (Ω). Power (P) was calculated as, P = IV.

3. Results and Discussion

3.1 FT-IR:

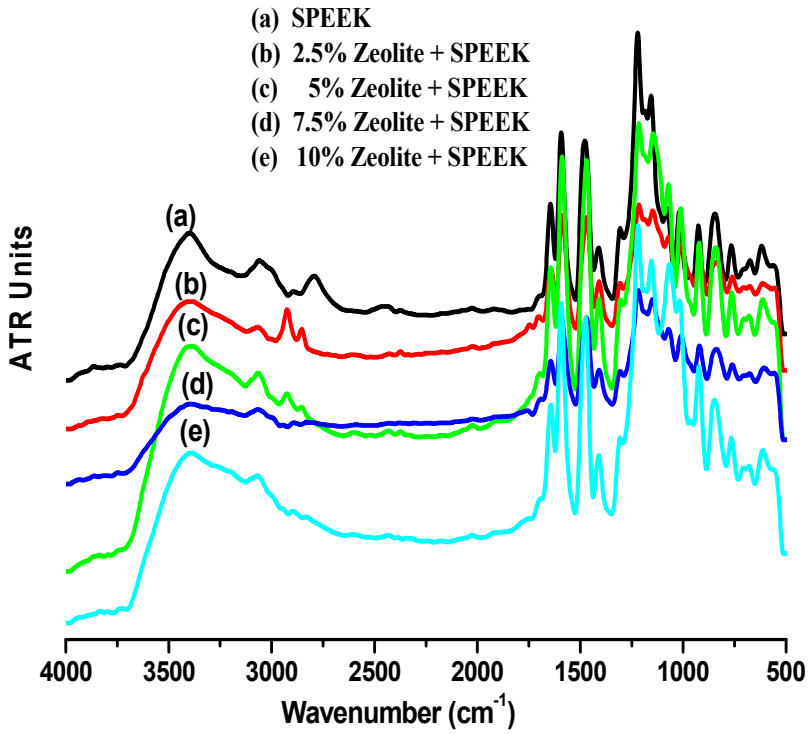

Fig. 1 FT-IR spectra of SPEEK- Zeolite composite membranes

The FT-IR spectra of SPEEK polymer and zeolite added SPEEK composite membranes are shown in Figure 1. The SPEEK spectrum demonstrates a new vibration frequency due to the characteristics of the sulfonic acid group (—SO_3H). The board peak at 3460 cm^{-1} can be assigned to the O—H vibration of—SO_3H. The peak at 1255 cm^{-1} is assigned to the asymmetric stretching of O=S=O. The peaks at 1080, 1020 and 709 cm^{-1} represent the symmetric stretching of O=S=O, S=O and S—O respectively. These data confirm the successful sulfonation of the PEEK polymer backbone. For the hybrid membrane, the peaks at 802 cm^{-1} and 950 cm^{-1} are assigned to the stretching vibrations of Si-O-Si, AlO_4 and Si-OH network of silica, respectively [45–47] while the large peak around 1153 cm^{-1} are assigned to the stretching vibrations of Si O Si and Al O Al bonds. The presence of these vibration peaks confirms the existence of aluminosilicate in the hybrid membrane.

3.2 XRD:

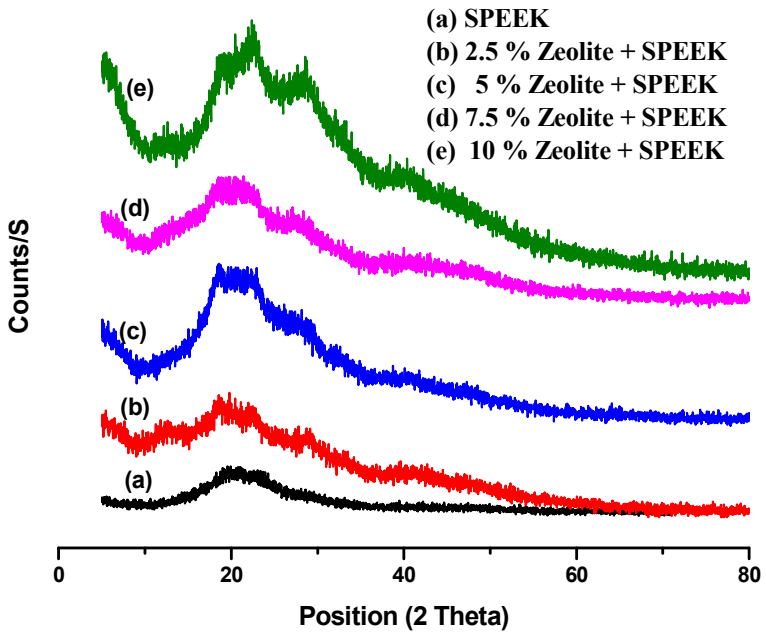

Fig.2. XRD patterns of SPEEK-Zeolite composite membranes

The X-ray diffraction measurement was performed to examine the crystallinity of the SPEEK and SPEEK/Zeolite composite membranes. Fig. 2 illustrates the X-ray diffraction pattern of the SPEEK/Zeolite membranes that were prepared with different zeolite content (Wt. %). It is clearly seen that the SPEEK polymer exhibits a semi crystalline structure with a huge peak at a 2θ angle of 19-20^{o}. The same peaks are also clearly observed for various Zeolite/SPEEK composite membranes in Fig. 2. It can be seen that the peak intensity at 2θ of 19-20 in the SPEEK/Zeolite composite membranes with different weight percentage of Zeolite was reduced as compared with that of virgin SPEEK polymer. Among various membrane samples, 7.5% Zeolite + SPEEK showed the lowest intensity at 19-20^{o}, which means that this membrane has the lowest crystallinity. The low crystallinity reveals that more amorphous phase exists in this membrane (7.5% Zeolite + SPEEK), indicating that the structure of the membrane is more

disordered due to more uniform mixing of SPEEK and Zeolite. Good mixing of SPEEK and zeolite is useful for the enhancement of ionic conductivity [48–50].

Table 1: Properties of Nafion and SPEEK membranes

Membrane Specification	Nafion	SPEEK
Thickness (mm)	0.019	0.018
Water Uptake (%)	22	15.83
IEC (milliequiv/g)	1.23	1.47
Proton Conductivity (x 10^{-2} S/cm)	2.0	0.148
Oxygen mass transfer Coefficient (K_o) (cm/s)	8 x 10^{-5}	4 x 10^{-6}

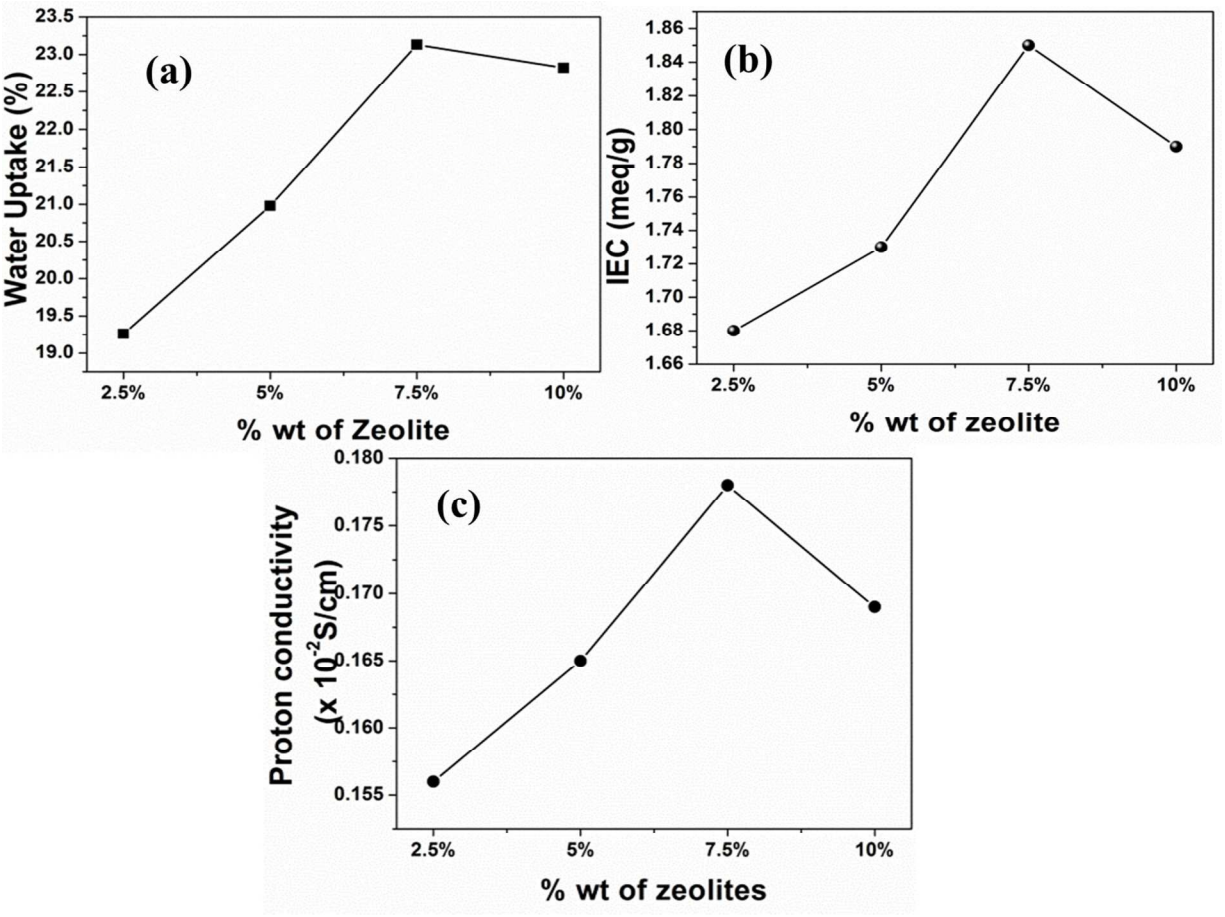

Fig. 3 (a) Water uptake, (b) IEC and (c) Proton conductivity of Zeolite + SPEEK composites

Water absorption capacity of the dry composite membranes showed increased tendency with increase in the addition of Zeolite (Fig 3 (a) this is because, zeolite structure consists of 3D connected pores having strong polarity, which can adsorb water well. It is found that composite membrane can adsorb higher water content than SPEEK membrane. Since water acts as a channel (mediator) for the ionic movement in polymer chain, increase in water absorption in turn increase the ionic and proton conductivity of the membranes. The ion-exchange capacities (IEC) of the fabricated membranes are presented in Fig. 3(b). Similar to water uptake, the addition of zeolite in SPEEK also increases the IEC of the composite membrane much higher than that of pure Nafion and SPEEK membrane.

Fig. 3(c) shows the proton conductivity of the composite membranes under controlled relative humidity (99.9%), at room temperature. The addition of zeolite enhances the proton conductivity compared to SPEEK membrane. However, above 7.5 % zeolite the conductivity declines with the incorporated amount. When large amount of zeolite was dispersed inside the polymer matrix, it might reach the limitation of uniform dispersion and started to agglomerate creating some voids among the clusters, which disrupt the continuum of sulfonic group clusters that are responsible for the proton motion in the sulfonated membrane. This improved conductivity of the composite membranes may come from the hydration inside the 3D channels of zeolite. The hydrated water enhances the motion of proton or hydronium ion via the exchange of proton between hydronium ion and water molecule [51,52]**.** The observed water uptake and proton conductivity results of study was in good agreement with the study made by Devrim and Albostan[53]**.**

3.3 Scanning Electron Microscopy:

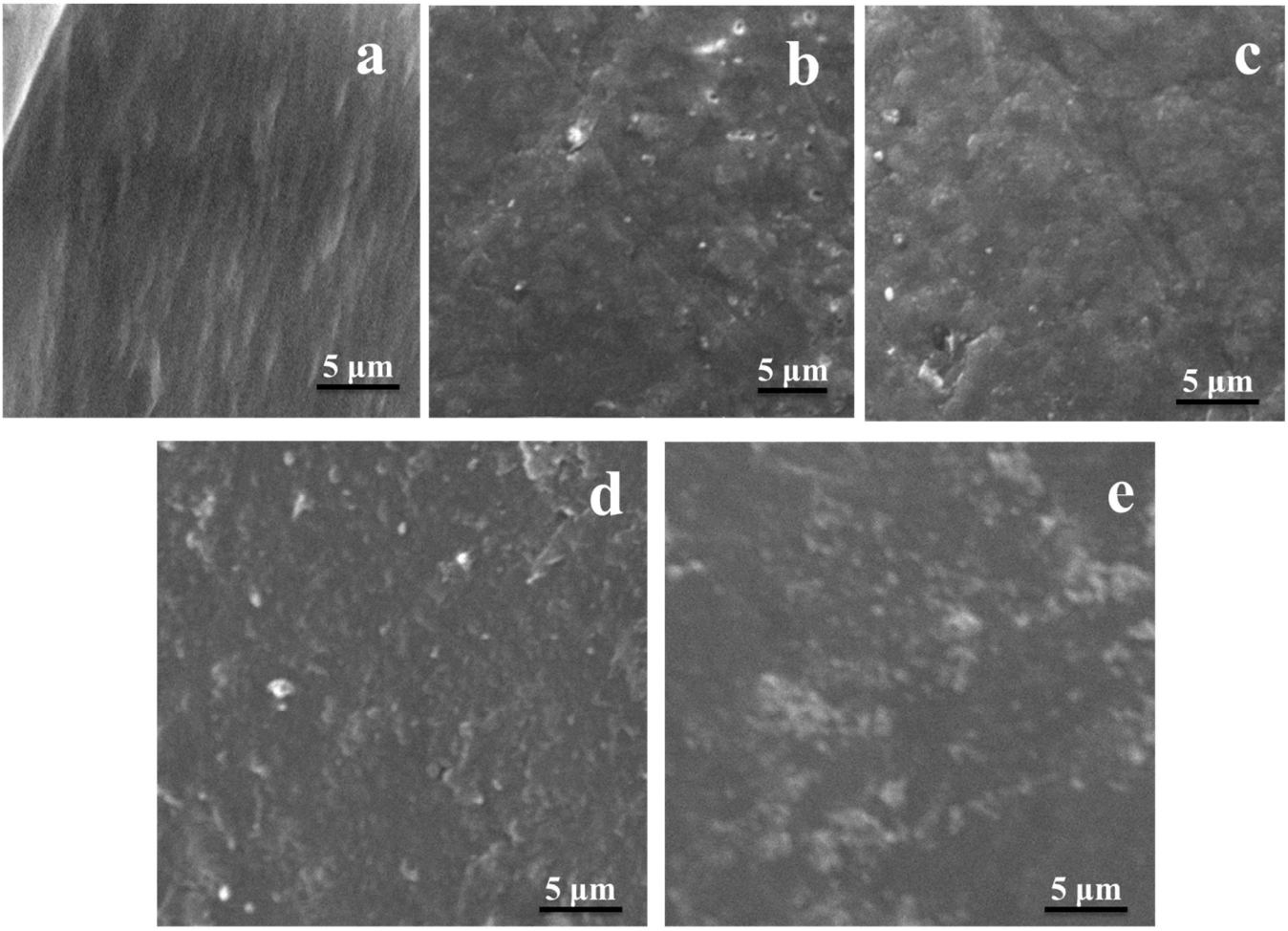

Fig. 3 SEM images of (a) SPEEK, (b) 2.5%, (c) 5 %, (d) 7.5% and (e) 10 % of SPEEK-Zeolite composite membranes

Fig. 3 shows some representative surface SEM micrographs of the SPEEK/faujasite composite membranes having various faujasite loading. The surface morphology of the composite membranes are uniform and non-porous with uniform dispersion of nano fillers. The image also confirmed the presence of zeolite particles on the surface of the polymer matrix. The dark region and white spots represent the SPEEK matrix and the faujasite particles respectively. As expected, the aggregation of zeolite particles increase with the zeolite content in the

polymeric matrix. On higher loadings, the same kind of particle aggregation on the surface of polymer matrix was observed on SPEEK, Nafion/zeolite systems[54,55].

3.4 Dissolved Oxygen Crossover:

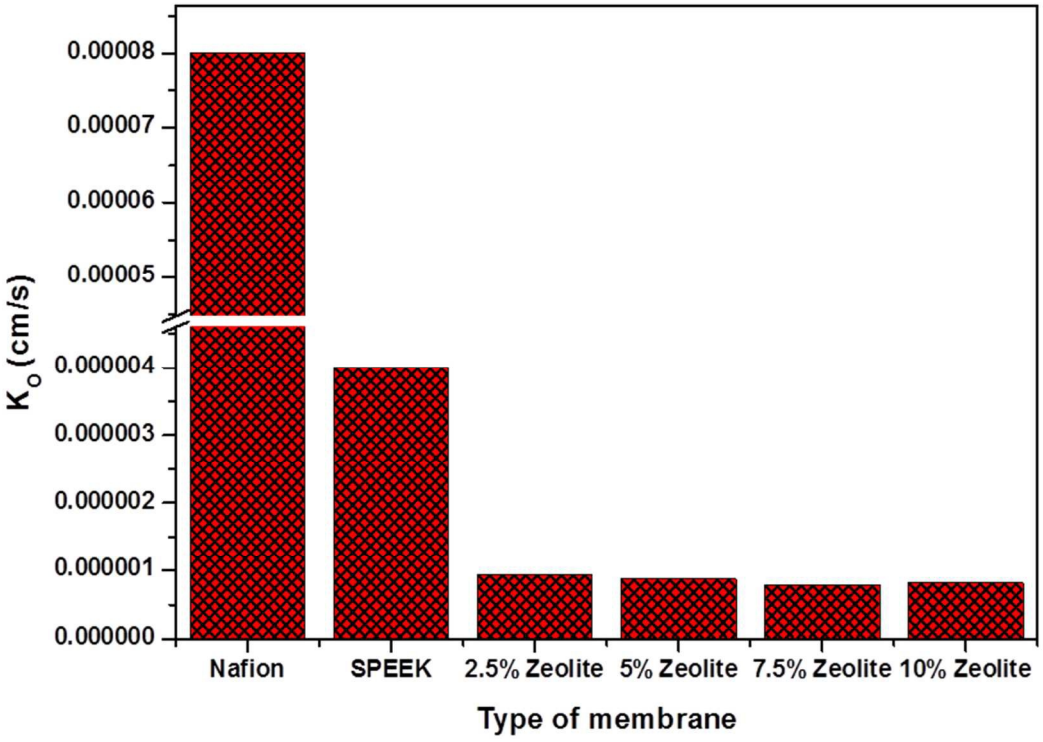

Fig. 4 Oxygen mass transfer coefficient of the membranes

One of the prime roles of membrane in MFC is to block the dissolved oxygen crossover towards anode chamber to maintain anode chamber oxygen free for the generation of proton and electrons from bacterial activities on degradable matters. The oxygen mass transfer coefficient of the membranes is shown in figure 4. From the figure, it was observed that SPEEK and all the zeolite incorporated SPEEK membranes showed one order less oxygen mass transfer coefficient (Ko) compared to that of Nafion 117® membrane. It was also observed that oxygen mass transfer coefficient rate of the composite membranes decreased with increase in zeolite content on SPEEK. This decreased oxygen mass transfer coefficient was due to the increased density of polymer matrix in presence of zeolite, which has showed strong resistance to oxygen flow

compared to that of SPEEK and Nafion membranes. 7.5% zeolite + SPEEK composite membrane showed less Ko of 0.79 x 10^{-6} cm/s among other prepared composite membranes, SPEEK and Nafion. The observed result of this study was in good agreement with the study made by Leong et al with SPEEK/graphene oxide[24] and Paisan et al with Nafion/faujasite for hydrogen fuel cells[56]. The oxygen mass transfer coefficient of membrane is an important factor in maintaining anaerobic environment and hence, it should be less for the improved performance of microbial fuel cell in terms of power density generation.

3.5 Surface roughness:

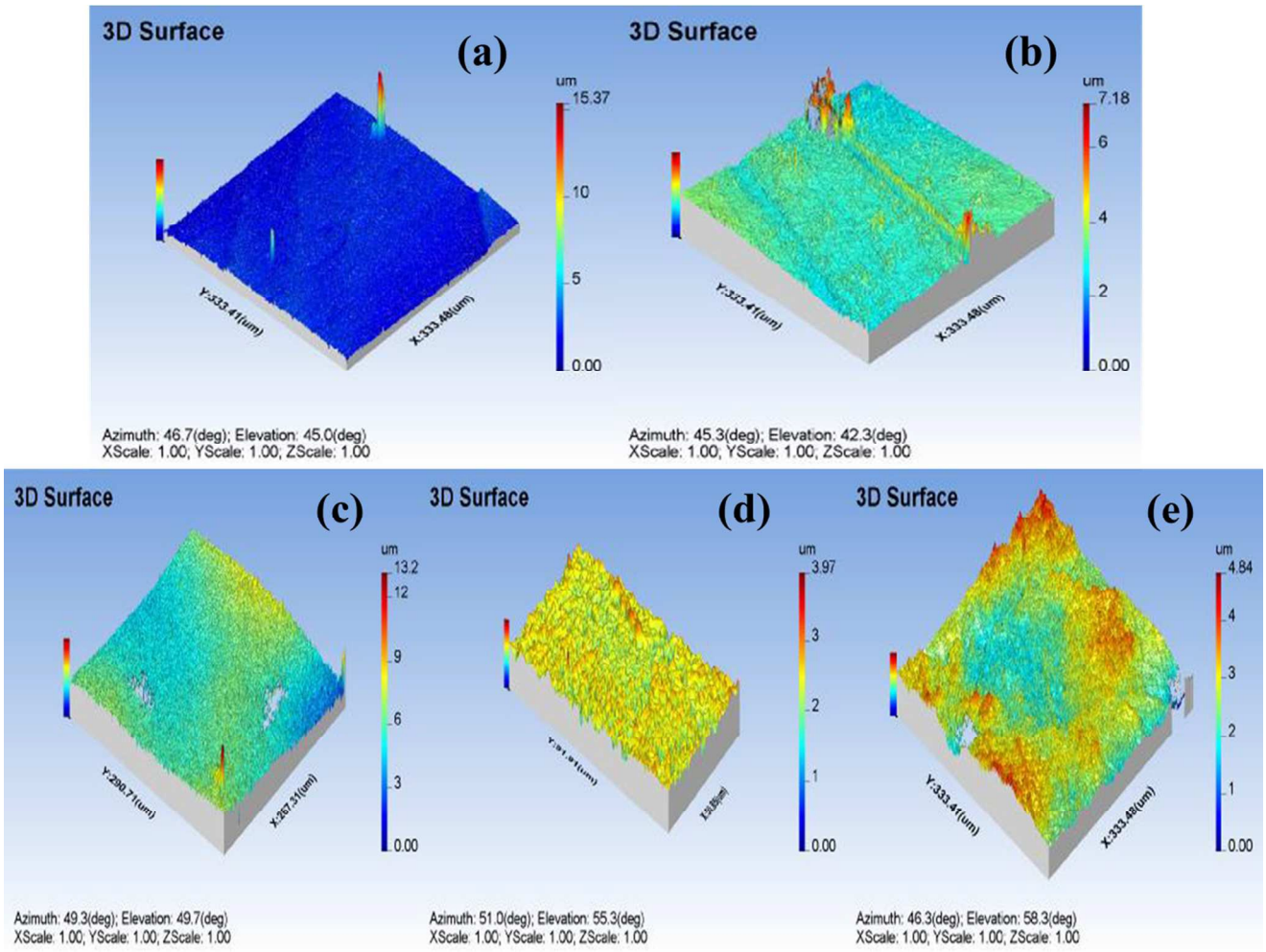

Fig. 5 Surface roughness images of (a) SPEEK, (b) 2.5%, (c) 5%, (d) 7.5% and (e) 10 % SPEEK- Zeolite composite membranes.

The surface roughness images of the prepared composite membranes are shown in Fig. 5. From the profilometer analysis, it can be concluded that the roughness of SPEEK membrane was less as compared to that of other membranes in the presence of zeolite which was in agreement with Lim et al [20]. It is observed that the roughness of the composite membrane increased with increase in zeolite weight as shown in Table 2 and similar kind of observation was recorded with PES/Fe_3O_4 composite membranes[22]. It is generally known that high roughness of a membrane increases the surface area of the membrane and leads to the formation of thin biofilms on the surface reduces the oxygen crossover from the cathodic chamber to the anodic chamber, which also enriches the anodic aerobic environment thus increasing the efficiency of the MFC. Hence, from the results of the surface roughness study, it could be expected that the power density of SPEEK-zeolite membranes would increase with higher percentages of zeolites.

Table 2: Surface Roughness of Membranes

Membrane	Average Surface Roughness (µm)
Nafion 117	0.097
SPEEK	0.110
2.5 % Zeolite + SPEEK	0.118
5 % Zeolite + SPEEK	0.123
7.5 % Zeolite + SPEEK	0.138
10 % Zeolite + SPEEK	0.165

3.6 Cations transport through membrane:

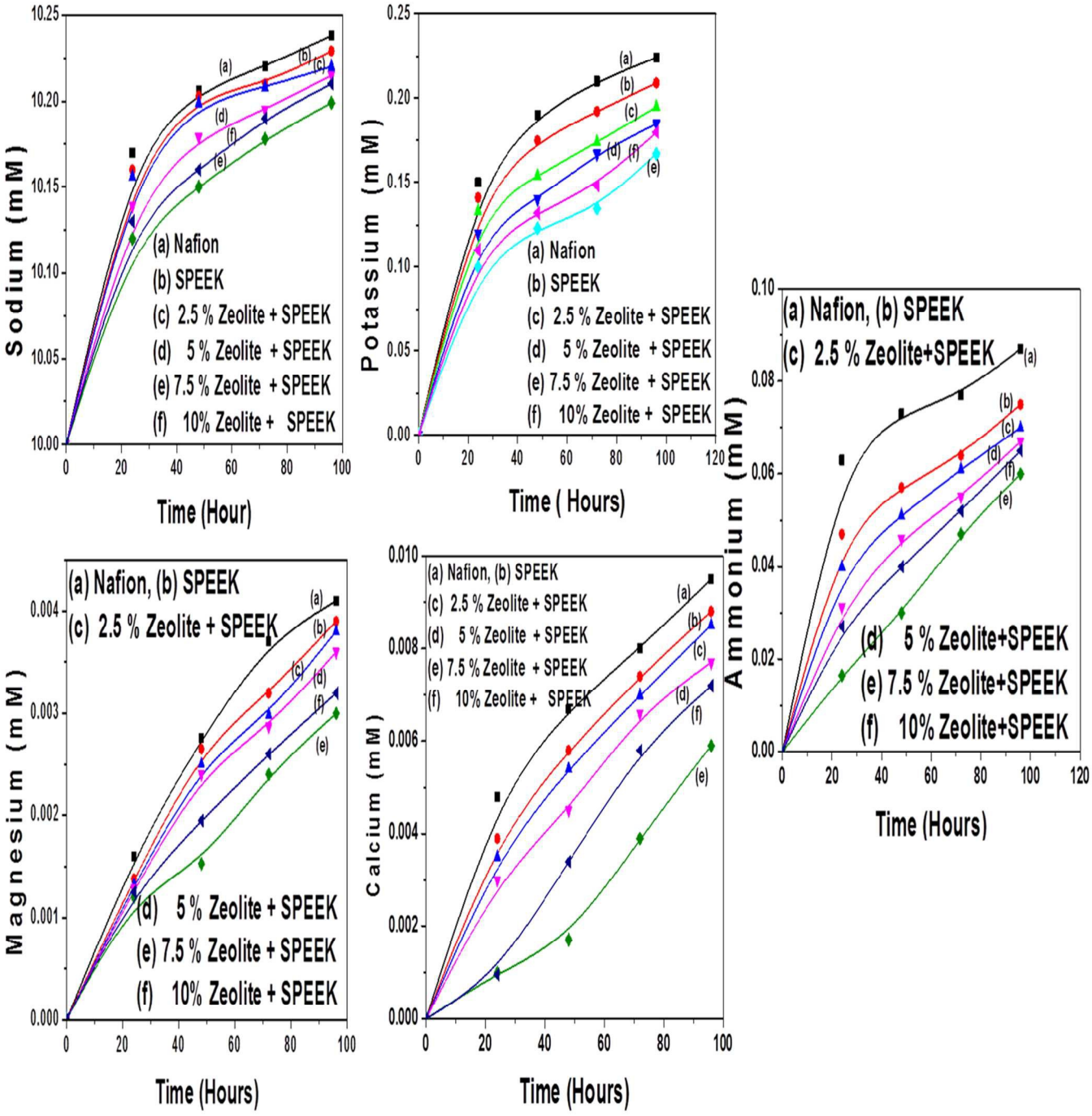

Fig. 6. Development of the cation concentrations (Na^+, K^+, NH_4^+, Ca^{2+}, and Mg^{2+}) in cathode chamber of a microbial fuel cell.

Other cations transport through the prepared membrane was studied in order to understand and maintain the performance of MFC on a longer run. The increased concentrations of the dominantly present cation species (Na^+, K^+, NH_4^+, Ca^{2+} and Mg^{2+}) in the cathode chamber during the 96 h experimental run was lower for zeolite - SPEEK composite membranes than Nafion and SPEEK membranes which was evidenced from the fig 6. The results clearly depict that Nafion membrane has higher cation transport than other composite membranes and 7.5% Zeolite + SPEEK composite membrane showed the least cation transport compared to all. This kind of cation separation by zeolite relies primarily on the size exclusion (steric) effect enabled by the zeolite's uniform sub nanometer pore sizes, in such case large hydration metal ions in aqueous solution cannot penetrate through it. The ion selective property of zeolite membranes has been already used as separators for brine desalination[57] and proton conduction in redox flow batteries[58,59]. The presence of uniform channels in such zeolites permits the small hydronium ions to diffuse through it but is impermeable to the large hydrated multivalent ions due to steric effects. In aqueous solution, metal ions on attraction with water molecules are hydrated. Depending upon the charge on metal ion the size of hydrated metal ions gets altered [60]. Unlike the metal ions, proton exists in the form of H_3O^+ (hydronium) in aqueous media. The H_3O^+ has three identical 'H–O' bonds making it a polyatomic cation with very small charge density that results in no definable hydration shell. The kinetic size of H_3O^+ is thus close to water molecule and is much smaller than the sizes of hydrated metal ions[57]. Therefore, zeolite based membranes have the potential to function as proton-selective ion exchange membranes. The passage of large hydrated metal ions through the composite membrane was restricted due to the resistance to the movement of hydrated ions through the porous structure of zeolites. This was reflected in the study, which showed less cation transport through the zeolite SPEEK membranes than that of

Nafion and SPEEK. This kind of larger molecule formation hinders the easy transport of metal ions through the ion exchange membranes[58] and showed less cationic (Na^+, K^+, NH_4^+, Ca^{2+} and Mg^{2+}) transport through the membrane. Hence, the addition of zeolite nano particle acts as barrier to cations and showed less crossover than Nafion and SPEEK membranes. The less cation transport in composite membranes would result in less organic (salt) precipitate on membrane, which in turn will result in less membrane fouling and hence a better fuel cell performance [28].

3.7 MFC Performance:

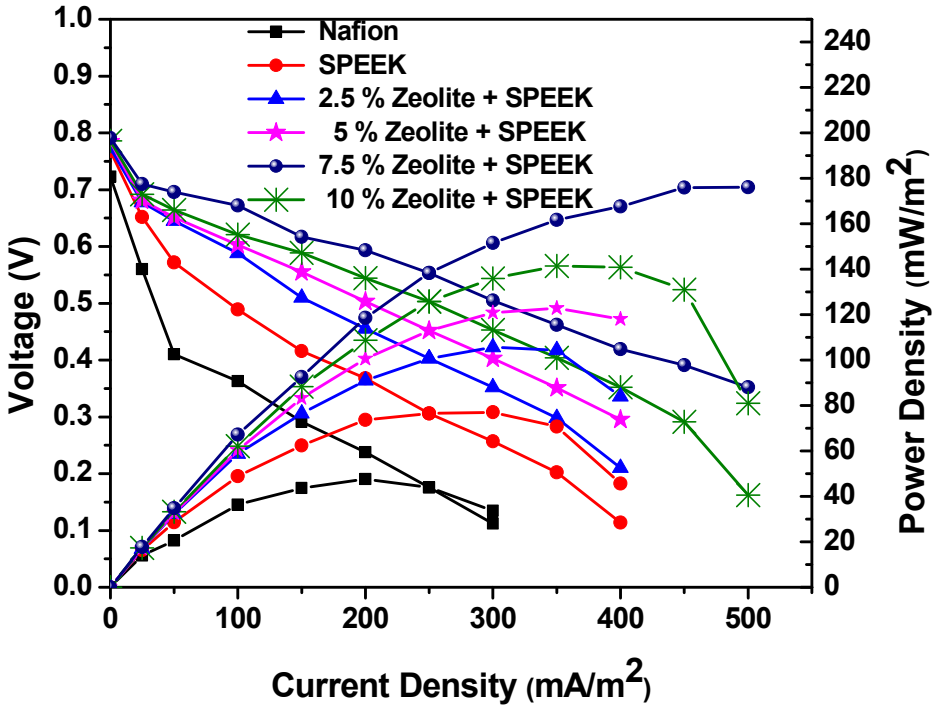

Fig. 7. Polarization curves of Nafion, SPEEK, 2.5%, (b) 5%, (c) 7.5%, (d) 10% SPEEK-Zeolite composite membranes

The performance of the prepared composite membranes in single chamber MFC is shown in Fig. 7. The main objective of this present study is to determine the significant impact of

zeolite particles in the improvement of SPEEK properties such as ion exchange capacity, proton conductivity, oxygen crossover and transport of other cations that are important to be an efficient electrolyte in MFCs operation. The prepared composite membranes showed higher percentage of columbic efficiency of 68%, 71%, 74% and 73% for composites with 2.5%, 5%, 7.5% and 10% of Zeolite by weight respectively compared to that of Nafion (47%) and SPEEK (64%) due to the efficient conversion of substrate molecules into proton, electron for the generation of electricity. The results showed that composite membranes showed better properties than that of Nafion and SPEEK membranes, which were, evidenced from oxygen crossover, IEC and proton conductivity data. SPEEK/Zeolite composite membranes showed higher power density values in particular, 7.5% Zeolite + SPEEK showed higher power density (176 mW/m^2) and current density (500 mA/m^2) than that of Nafion (47.6 mW/m^2 and 200 mA/m^2) and SPEEK (77 mW/m^2 and 300 mA/m^2). Such a better performance primarily depends upon i) maintaining strict anode anaerobic environment as a result of less oxygen crossover from cathode to anode, ii) with less other cation transport. In spite of the fact that Nafion shows better proton conductivity, it lacks in terms of the above, especially for MFC applications. When faujasite was loaded into the SPEEK matrix, it is found that the proton conductivity of the composite membrane increases with the increasing amount of Faujasite. The increased proton conductivity of composite membranes obtained with zeolite loading, was attributed to the water management and protons inside the connected 3D channels of the Faujasite [56] and restriction of large hydrated cations flow through the uniform zeolite pore structure. These protons acted as bridges for the proton transfer enhancing the proton conductivity of the hybrid membrane. On addition of the faujasite to SPEEK matrix, the increase in amorphous nature of the polymer composite membranes was observed and showed uniform mixing of nano fillers with that of polymer matrix, which helped for the improved ionic

conductivity. It is worth noting that with respect to the cost analysis, the cost of the composite polymer SPEEK/Zeolite (approximately 4-5 $/cm^2) is much lower when compared to the commercial membrane, Nafion (10 $/cm^2) [61].

4. Conclusion:

The advancements in the alternative membranes for MFC at relatively low cost requires membranes with targeted properties such as high ionic, proton conductivity, less oxygen crossover, preferable proton conduction more than that of commercial membranes. In this study, H-faujasite type zeolite was chosen for its proton conductivity with uniform pore size and structure. Based on the property of faujasite high efficiency composite membranes were developed at low cost with high proton conductivity, less oxygen and other cation transport property that resulted in higher power density output through MFC operation was achieved. The prepared composite membranes are suitable candidate for MFC application due to their superior properties compared to that of SPEEK and Nafion membranes.

Acknowledgement:

The authors thank the Department of Science and Technology (DST) India, for their financial support to carry out this work vide letter No. DST/TSG/AF/2010/09,dt.01-10-2010.

Reference:

1 V. D. Patil, D. B. Patil, M. B. Deshmukh and S. H. Pawar, *Int. J. Chem. Sci. Appl.*, 2011, **2**, 108–115.

2 N. a. Garcia-Gomez, I. Balderas-Renteria, D. I. Garcia-Gutierrez, H. a. Mosqueda and E. M. Sánchez, *Mater. Sci. Eng. B*, 2015, **193**, 130–136.

3 G. Gunasekaran, S. Chongdar, S. Naragoni, P. V. Rodrigues and R. Bobba, *Int. J. Hydrogen Energy*, 2011, **36**, 14914–14922.

4 S. Bakhshian, H. R. Kariminia and R. Roshandel, *Bioresour. Technol.*, 2011, **102**, 6761–6765.

5 Y. Sun, J. Zuo, L. Cui, Q. Deng and Y. Dang, *J. Gen. Appl. Microbiol.*, 2010, **56**, 19–29.

6 K. C. Wrighton, J. C. Thrash, R. a. Melnyk, J. P. Bigi, K. G. Byrne-Bailey, J. P. Remis, D. Schichnes, M. Auer, C. J. Chang and J. D. Coates, *Appl. Environ. Microbiol.*, 2011, **77**, 7633–7639.

7 K. Scott and C. Murano, *J. Chem. Technol. Biotechnol.*, 2007, **82**, 92–100.

8 W. Verstraete and K. Rabaey, *Environ. Sci. Technol.*, 2006, **40**, 5181–5192.

9 N. Venkatesan Prabhu and D. Sangeetha, *J. memb*, 2013, **435**, 92–98.

10 N. M. Nik Azmi, N. F. Ghazali, A. Fikri and M. A. Ali, *Adv. Mater. Res.*, 2015, **1113**, 823–827.

11 M. Wei, F. Harnisch, C. Vogt, J. Ahlheim, T. R. Neu and H. H. Richnow, *RSC Adv.*, 2015, **5**, 5321–5330.

12 and P. C. F.J. Fernandez, J. Lobato, J. Villasenor, M.A. Rodrigo and Abstract, in *Environment, Energy and Climate Change I: Environmental Chemistry of Pollutants and Wastes.*, 2014, pp. 273–303.

13 F. J. Hernández-Fernández, a. Pérez de los Ríos, F. Mateo-Ramírez, C. Godínez, L. J. Lozano-Blanco, J. I. Moreno and F. Tomás-Alonso, *Chem. Eng. J.*, 2015, **279**, 115–119.

14 V. N. Blagovesta Midyurova , Husein Yemendzhiev , Petko Tanev, *J. Chem. Technol. Metall.*, 2015, **50**, 543–550.

15 S. M. Daud, K. B. Hong, M. Ghasemi and W. R. W. Daud, *Bioresour. Technol.*, 2015.

16 N. Venkatesan Prabhu and D. Sangeetha, *Chem. Eng. J.*, 2014, **243**, 564–571.

17 N. Venkatesan Prabhu and D. Sangeetha, *J. Mater. Sci.*, 2015, **50**, 6302–6312.

18 S. Ayyaru and S. Dharmalingam, *Bioresour. Technol.*, 2011, **102**, 11167–11171.

19 W.-W. Li, G.-P. Sheng, X.-W. Liu and H.-Q. Yu, *Bioresour. Technol.*, 2011, **102**, 244–252.

20 S. S. Lim, W. R. W. Daud, J. Md Jahim, M. Ghasemi, P. S. Chong and M. Ismail, *Int. J. Hydrogen Energy*, 2012, **37**, 11409–11424.

21 S. Ayyaru and S. Dharmalingam, *RSC Adv.*, 2013, **3**, 25243.

22 M. Rahimnejad, M. Ghasemi, G. D. Najafpour, M. Ismail, a. W. Mohammad, a. a. Ghoreyshi and S. H. a. Hassan, *Electrochim. Acta*, 2011, **85**, 700–706.

23 G. Rambabu and S. D. Bhat, *Electrochim. Acta*, 2015, **176**, 657–669.

24 J. X. Leong, W. R. W. Daud, M. Ghasemi, A. Ahmad, M. Ismail and K. Ben Liew, *Int. J. Hydrogen Energy*, 2015, 1–11.

25 M. Ghasemi, S. Shahgaldi, M. Ismail, Z. Yaakob and W. R. W. Daud, *Chem. Eng. J.*, 2012, **184**, 82–89.

26 S. Shahgaldi, M. Ghasemi, W. R. Wan Daud, Z. Yaakob, M. Sedighi, J. Alam and A. F. Ismail, *Fuel Process. Technol.*, 2014, **124**, 290–295.

27 A. Mayahi, H. Ilbeygi, A. F. Ismail, J. Jaafar, W. R. W. Daud, D. Emadzadeh, E. Shamsaei, D. Martin, M. Rahbari-Sisakht, M. Ghasemi and J. Zaidi, *J. Chem. Technol. Biotechnol.*, 2015, **90**, 641–647.

28 N. Venkatesan Prabhu and D. Sangeetha, *J. Memb. Sci.*, 2015, **492**, 518–527.

29 T. Sancho, J. Soler and M. P. Pina, *J. Power Sources*, 2007, **169**, 92–97.

30 A. Dyer and M. Zubair, *Microporous Mesoporous Mater.*, 1998, **22**, 135–150.

31 R. T. Pabalan and F. P. Bertetti, *Rev. Mineral. Geochemistry*, 2001, **45**, 453–518.

32 V. Tricoli and F. Nannetti, *Electrochim. Acta*, 2003, **48**, 2625–2633.

33 V. Felice and A. C. Tavares, *Solid State Ionics*, 2011, **194**, 53–61.

34 I. Daems, P. Leflaive, A. Méthivier, G. V. Baron and J. F. M. Denayer, *Microporous Mesoporous Mater.*, 2006, **96**, 149–156.

35 H. García and H. D. Roth, *Chem. Rev.*, 2002, **102**, 3947–4007.

36 Z. Zhang, F. Désilets, V. Felice, B. Mecheri, S. Licoccia and A. C. Tavares, *J. Power Sources*, 2011, **196**, 9176–9187.

37 S. Guhan, N. Venkatesan Prabhu and D. Sangeetha, *Polym. Sci. Ser. A*, 2011, **53**, 1159–1166.

38 O. Lefebvre, Y. Shen, Z. Tan, A. Uzabiaga, I. S. Chang and H. Y. Ng, *Bioresour. Technol.*, 2011, **102**, 6291–6294.

39 R. a Rozendal, H. V. M. Hamelers and C. J. N. Buisman, *Environ. Sci. Technol.*, 2006, **40**, 5206–5211.

40 B. Min, S. Cheng and B. E. Logan, *Water Res.*, 2005, **39**, 1675–1686.

41 T. Zhang, Y. Zeng, S. Chen, X. Ai and H. Yang, *Electrochem. commun.*, 2007, **9**, 349–353.

42 T. Zhang, C. Cui, S. Chen, H. Yang and P. Shen, *Electrochem. commun.*, 2008, **10**, 293–297.

43 T. Zhang, C. Cui, S. Chen, X. Ai, H. Yang, P. Shen and Z. Peng, *Chem. Commun. (Camb).*, 2006, 2257–2259.

44 S. Cheng, H. Liu and B. E. Logan, *Electrochem. commun.*, 2006, **8**, 489–494.

45 a. K. Sahu, G. Selvarani, S. Pitchumani, P. Sridhar and a. K. Shukla, *J. Electrochem. Soc.*, 2007, **154**, B123.

46 K. T. Adjemian, S. J. Lee, S. Srinivasan, J. Benziger and a. B. Bocarsly, *J. Electrochem. Soc.*, 2002, **149**, A256.

47 S. Cavalu, V. Simon, F. Bănică and C. Deleanu, *Rom. j.Biophys.*, **17**, 237–245.

48 E. D. Wang, T. S. Zhao and W. W. Yang, *Int. J. Hydrogen Energy*, 2010, **35**, 2183–2189.

49 A. Ebadi Amooghin, M. Omidkhah and A. Kargari, *RSC Adv.*, 2014, **5**, 8552–8565.

50 W. Li, Y. Xing, Y. Wu, J. Wang, L. Chen, G. Yang and B. Tang, *Electrochim. Acta*, 2015, **151**, 289–296.

51 W. H. J. Hogarth, J. C. Diniz da Costa and G. Q. (Max. Lu, *J. Power Sources*, 2005, **142**, 223–237.

52 S. H. Kwak, T. H. Yang, C. S. Kim and K. H. Yoon, *Solid State Ionics*, 2003, **160**, 309–315.

53 Y. Devrim and A. Albostan, *Int. J. Hydrogen Energy*, 2015, 1–8.

54 J. Auimviriyavat, S. Changkhamchom and A. Sirivat, *Ind. Eng. Chem. Res.*, 2011, **50**, 12527–12533.

55 M. Lavorgna, L. Sansone, G. Scherillo, R. Gu and a. P. Baker, *Fuel Cells*, 2011, **11**, 801–813.

56 P. Kongkachuichay and S. Pimprom, *Chem. Eng. Res. Des.*, 2010, **88**, 496–500.

57 J. Dong, Z. Xu, S. Yang, S. Murad and K. R. Hinkle, *Curr. Opin. Chem. Eng.*, 2015, **8**, 15–20.

58 R. Yang, Z. Xu, S. Yang, I. Michos, L. F. Li, A. P. Angelopoulos and J. Dong, *J. Memb. Sci.*, 2014.

59 R. Yang, Z. Cao, S. Yang, I. Michos, Z. Xu and J. Dong, *J. Memb. Sci.*, 2015, **484**, 1–9.

60 J. KIELLAND, *PORSGRUNN, Norw.*, 1937, 58, 297–300.

61 M. Ghasemi, W. R. W. Daud, A. F. Ismail, Y. Jafari, M. Ismail, A. Mayahi and J. Othman, *Desalination*, 2013, **325**, 1–6.